UNCONVENTIONAL TESTER FOR THE VERIFICATION OF GTO-MODEL-PARAMETERS AND FOR THE INVESTIGATION OF THE CURRENT DENSITY DISTRIBUTION IN GTO TABLETS

Henry Güldner, Andreas Thiede
Dresden University of Technology, Chair of Power Electronics
Mommsenstr. 13, D-01062 Dresden
Phone +(0)351 4634303, Fax +(0)351 4637270

Hans-Joachim Schulze, Jakob Sigg, Johann Otto
Siemens AG, Corporate Research and Development Department, ZT KM 6
Otto-Hahn-Ring 6, D-81730 Munich, Phone +(0)89 63648654, Fax +(0)89 63648655

Lutz Göhler
University of Bundeswehr Munich
Werner-Heisenberg-Weg 39, D-85577 Neubiberg
Phone +(0)89 6004 3665, Fax +(0)89 6004 2223

Dieter Metzner
eupec GmbH + Co. KG
Schloßberg 10, D-91362 Pretzfeld, Phone +(0)9194 7340 88, Fax +(0)9194 7340 25

ABSTRACT - This paper describes the main features of an unconventional tester for high power semiconductor devices. Two application ranges are highlighted. The tester is used for the extraction of GTO parameters and their verification by measurements. The second field comprises the determination of the radial and azimuthal current density distribution of a GTO tablet. The results are compared with the carrier lifetime distribution.

1. INTRODUCTION

In the low voltage range of power electronics CAD packages already gained wide acceptance as tools in the development process. Physics-based models have been developed and can be applied for the investigation of modern circuit topologies. The generic models for power semiconductor devices have to parameterized for a specific component. The equipment for the parameter extraction routines are available in most power electronic laboratories.

At the high power end currents and voltages in the kA and kV range, respectively, have to handled. In this power regime there is not setup available for transient investigations. In the first part this paper describes the main features of such an universally applicalbe tester. It is designed to study the turn-on and turn-off characterisitics of high power semiconductor devices. The unique feature of the concept of this setup is the unconventional capacitance arrangement.

The second part analyzes the extraction of parameters for a 4,5kV/3,0kA GTO. By measuring at the same time the gate as well as the load currents and voltages a maximum of information is obtained about the device under test (DUT). The setup is also used to check the extracted parameter set by varying the current and voltage transients in a wide range.

High current GTO devices consist of Silicon chips with a large area (roughly 50cm^2). The inhomogenities across the wafer limit the switching capability of modern high power GTO components. Extending the established tester with further measuring facilities it can be applied to study the transient current density distribution across the device. The extension of the setup as well as the results are given in the fourth part.

2. TEST CIRCUIT

2.1. Background

This paper deals with a test circuit for investigating the switching capability of power semiconductors. It employs the booster principle and is able to generate blocking voltages up to 4kV and turn-off currents up to 4kA. The dual-pulse technique is used for testing. The objective was to fabricate this tester at minimum cost. Thus the number of power semiconductors used and the expenditure on passive components had to be minimized. There was therefore no need to consider the two- or four-quadrant converter topologies. This left the choice between

- the conventional dc-chopper supplying an inductive load or
- a booster circuit, which operates on a capacitive load.

Both circuits need only two main valves in the power bench. Thus the expenditures for the passive components remains as deciding factor. If one calculates the size of necessary inductances and capacities for both circuits,

then the surprising result is, that the test circuit represented in the Fig. 1 needs less than 50% of the capacity of the classical dc-chopper circuit [1].

$$\frac{L_{buck}}{L_{boost}} = 1 - \frac{\Delta u}{100} \tag{1}$$

$$\frac{C_{buck}}{C_{boost}} = \frac{50 \left(1 - \frac{\Delta u}{100}\right)}{\left(k_r^2 \, \Delta u + \Delta i - \frac{\Delta i^2}{200}\right)} \tag{2}$$

For $\Delta u = \Delta i = 10\%$ as well as $k_r = 1.1$ arises:

$$\frac{L_{buck}}{L_{boost}} = 0.9 \quad ; \quad \frac{C_{buck}}{C_{boost}} = 2.1$$

With the following meanings:

Δu	-	relative blocking voltage change during pulse sequence
Δi	-	percental current change during second on-state
k_r	-	coefficient to consider the resistance components of the resonant circuit.

However, the expenditure on inductances is approximately equivalent in both circuits. Since, aside from the power semiconductors, the capacitors represent the major cost factor, these realizations led to the decision to use the booster circuit for the test equipment. Apart from the cost factor, this circuit proves to be short-circuit-proof in the event of DUT failure.

2.2. Functionality

The circuit diagram of the tester is shown in Fig. 1. The special feature of this circuit compared to the dc-chopper is the distribution of the dual function of capacitance Ċ to two capacitors C1 and C2. Capacitor C1 has the sole function of supplying the booster current source L1 with energy (Fig. 2).

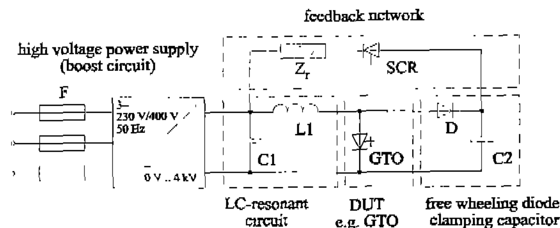

Fig. 1 Main circuit

By appropriate adjustment of resonant circuit elements C1 and L1, the switch-off current corresponds to the amplitude of the current oscillation. No problems are expected with rapidly increasing short-circuit currents which are difficult to control in the event of DUT failure. Capacitor C2 operates as the load for the booster which supplies the off-state voltage during the free-wheel periods for the DUT. In order to avoid unacceptably high off-state voltages in the case of a purely capacitive load, an additional feedback network (Fig. 1) was introduced. The thyristor SCR is triggered even before the first turn-off of the DUT occurs. On the one hand, part of the energy stored in C2 arrives via the feedback network at C1. On the other hand, the free-wheel circuit L1-D-SCR-Zr-L1 closes mainly via this leg while the DUT is switched off, which means that the energy stored in L1 no longer results in further charging of C2. The losses in semiconductors and resistors must be delivered up to the next double pulse by the power supply, which also consists of a booster circuit. A detailed analytical description of the test circuit is given in [1].

3. EXTRACTION OF GTO MODEL PARAMETERS

Depending on the simulation objective, models with different accuracy levels are required. Since a higher accuracy requires more computation time and a more technology-based parameter set, model level selection is a compromise between quality, calculation time and efforts necessary for parameter determination.

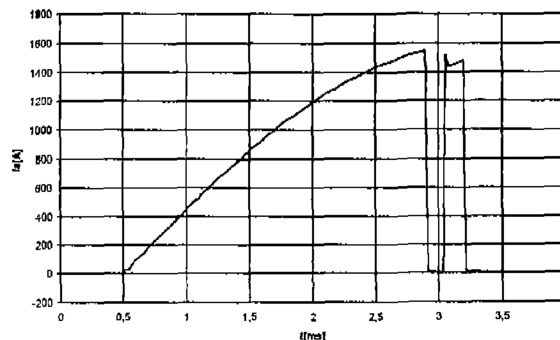

Fig. 2 Typical resonant current pulse

The more information the user wants to obtain from a simulation in a given time, the more carefully all inputs have to be checked and the more difficult the compromise can look. As already mentioned, an important point is the model level. For example, a simple switch model or a static description of the power semiconductor devices can never predict the dynamic stress, for instance, in a quasi-resonant ZCS circuit incorporating a Power MOSFET [5]. Only a more precise, dynamic model is able to support these data. The need for parameter determination is common to all models. However, the complexity of these procedures is the main deciding factor for acceptance in practice. The test circuit presented in this paper considerably simplifies parameter extraction for most

physics-based models. These advantages are demonstrated below using an example.

3.1. Extraction of minority carrier lifetime in the n-base

It is well-known, that the high-level carrier lifetime in a GTO without an excessively high degree of anode shorting can be calculated from the tail current time constants at various loads.

In our example a 4.5kV/3kA GTO is used as the device under test (DUT). The load current varies between 100A and 500A in increments of 100A.

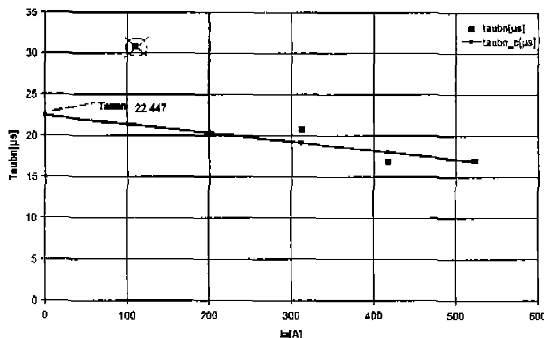

Fig. 3: τ_{pbn} as a function of the anode current

For each of these values the extracted time constant is plotted in Fig. 3.

Extrapolating this characteristic to I_a=0 provides the high-level injection lifetime in the n-base, which is approximately twice the value of the desired minority carrier lifetime. From many experiments, device manufacturer found a value of τ_{pbn} in the range (10..20)µs. In comparison to this, it can be stated that our method produces a reasonable value (τ_{pbn}=11.2us).

Additionally, some other important parameters for physics-based models can be identified using our test circuit:

A	-	active area
wbn	-	width of n-base
wbp	-	width of p-base
wep	-	width of p-emitter
wen	-	width of n-emitter
Nbn	-	doping of n-base
Nbp	-	peak doping of p-base (near junction to n-emitter)
Nep	-	peak doping of p-emitter
Nen	-	peak doping of n-emitter
bvgk	-	gate-cathode breakdown voltage
bvga	-	gate-anode breakdown voltage
taupbn	-	minority carrier lifetime in n-base
taumbp	-	minority carrier lifetime in p-base
rs	-	resistance of anode shorts
Isep	-	saturation current for description of electron injection into p-emitter
Isen	-	saturation current for description of hole injection into n-emitter

The measurement of currents, voltages and junction capacitances, i.e. electrical quantities, means that there is no destruction of the DUT. Further information on the sequence to be performed is given in [2] and [9] and is omitted here for reasons of complexity and available space.

3.2. Verification of a Physics-Based Model

Using the proposed setup, verification of models of various GTO components can be performed easily. To demonstrate this

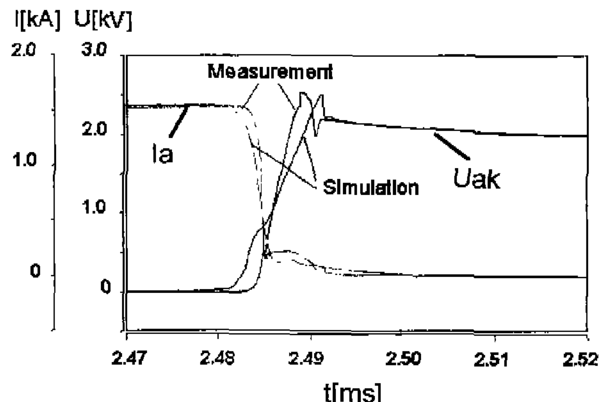

Fig. 4: GTO turn off - measurement and simulation

feature, a turn-off process of the railway GTO at 1.5kA is compared with a circuit simulation in SABER (Fig. 4) [3]. The two curves show a convincing agreement, confirming good model quality under the given circuit conditions. One could now check the model at different voltage and current levels to evaluate the overall quality. However, in order to demonstrate the advantage of using the new circuit, one example would appear to suffice.

4. CURRENT DENSITY DISTRIBUTION OF A GTO

Inhomogenities in the silicon starting material (cycle 0) on the one hand and inhomogenities, which are due to the GTO process technology (wafer processing), on the other, result in a limitation of the switching capability of modern high-power GTO thyristors. In order to be able to determine the causes for this, the local and transient current density distribution of the GTO must be recognizable. The following tasks are therefore involved:

a) Evaluation and verification of measuring techniques for the local and transient current density distribution in the GTO
b) Determination of inhomogeneities in the current density distribution using the abovementioned measuring technique, particularly in respect of any physical boundary conditions and influencing factors (electrical, thermal, mechanical, etc.)
c) Determination of the reason for these inhomogeneities

and verification of all the latter by means of special measurements and 3D simulations.

d) Elimination of the determined reasons by influencing the technological processes (cycle 0 and wafer processing, packaging, handling etc.)
e) Verification of the effectivness of the process optimization by new measurements of the current density distribution.

The development of non-destructive measuring methods is acquiring ever increasing importance. In order to obtain realistic results, the selected method must, in addition, not influence the elementary device behavior. Two methods which are being used in the described tester are detailed below.

4.1. Measurement of the radial current density distribution

The measurement of the radial current density distribution with concentric rogowski coils employs zoning of the GTO cathode into several cathode finger rings [4]. Fig. 5 shows the principle of the measuring instrument. Each rogowski coil of the test capsule measures the current component of all enclosed cathode finger rings. In addition (in GTOs with ring gate), the three outside coils measure the gate current which must be taken into account for the subsequent calculation.

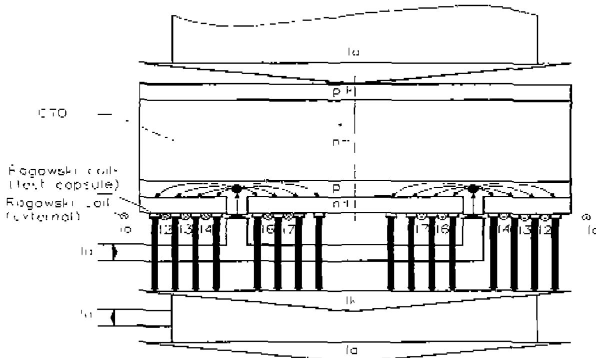

Fig. 5: Measurement of radial current density distribution

Under these premises the following formulations are obtained for the cathode current components of individual finger rings or pairs of finger rings:

$$\begin{aligned} I_{KR1} &= I_A - I_2 \\ I_{KR2} &= I_2 - I_3 \\ I_{KR3} &= I_3 - I_4 \\ I_{KR4+5} &= I_4 - I_6 + I_G \\ I_{KR6} &= I_6 - I_7 \\ I_{KR7+8} &= I_7 \end{aligned} \quad (3)$$

I_{KRi} is the cathode current of one or two finger rings, I_i denotes the current measured by the rogowski coils, I_A is the anode current and I_G is the gate current.

The appropriate current densities are calculated using the well-known relationship:

$$s_{KR\nu\mu} = \frac{di_{KR\nu\mu}}{dA_{KR\nu}} \approx \frac{i_{KR\nu\mu}}{A_{KR\nu}}; \ \nu = 1...6 \quad (4).$$

Where s_{KR} denotes the transient current density of one or two cathode finger rings and A_{KR} the emitter area of the corresponding finger ring or ring pair.

Using this principle, only the the cathode current density in finger rings or pairs of finger rings can be determined.

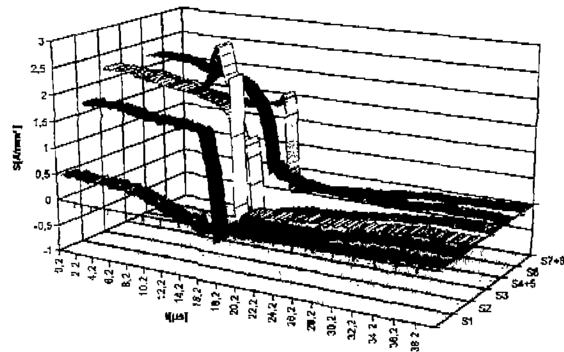

Fig. 6 Measurement of radial current density distribution during turn off

The result of a measurement of the radial current density distribution is shown in Fig. 6. Both the different current density distribution under steady state conditions and the current redistribution during turn-off are clearly detectable.

4.2. Determination of the azimuthal current density distribution by $\vec{H}$-field measurements

The magnetic field strength is measured by small pickup coils along an aperture around the GTO device. Current changes in the GTO cause a voltage to be induced in the coils, from which, considering the coil design, the vector $\vec{H}$ of the magnetic field strength can be calculated. Different current densities in the GTO cause a deviation of the field strength signal from the expected homogeneous dependence. The degree of deviation provides information about the magnitude of the inhomogeneity [6]-[8]. With the help of mathematical methods it is possible, as part of a generally extensive analysis, to calculate the most probable current density distribution in the element which could have caused such a magnetic field strength differing from a homogeneous progression. Precise knowledge of the processes occurring during turn-on and turn-off in the element is not necessary for this purpose. The wafer here is understood rather as an observation area with conductivity varying in place and time.

To calculate the current density distribution in the subdivided observation area, the voltage induced in the pickup coils is treated as a superimposition of all voltage components resulting from current changes in discrete filaments of the observation area. This gives:

$$u_{ma\eta} = \sum_{\xi} u_{ma\xi\eta} = \sum_{\xi} M_{ma\xi\eta} \frac{di_{a\xi}}{dt} \; ; \xi \in \{N,1...n\} \qquad (5)$$

n being the number of discrete filaments. If this equation is integrated, the following is obtained:

$$\int u_{ma\eta} dt = \sum_{\xi} M_{ma\xi\eta} i_{a\xi} + C \quad ; \quad M_{ma\xi\eta} = \underbrace{K}_{Sensor} \cdot \underbrace{G_{ma\xi\eta}}_{Geometry} \qquad (6).$$

The mutual inductance is the product of a factor K reflecting the properties of the pickup coil, and a geometric factor G. By introducing the magnetic field strength and dividing by K, we get:

$$H_{\eta}(t) = \sum_{\xi} H_{\xi\eta}(t) = \frac{\int u_{ma\eta} dt}{K} = \sum_{\xi} G_{ma\xi\eta} i_{a\xi}(t) \quad ; \quad K \approx \mu w_s A_s \qquad (7).$$

The results obtained for $\bar{H}$ can be easily checked by Ampere's rule.

With the help of the Biot-Sarvard law, it is possible to calculate the geometric factors G for each discrete filament of the observation area. This calculation can be made in advance of the measurements, as the geometric data of the measuring system and the DUT are generally known. On the basis of

$$d\bar{H}(t) = \sum_{\xi} i_{a\xi}(t) \cdot \frac{d\vec{s} \times \vec{r}_{\xi}}{4\pi r_{\xi}^{3}} \qquad (8)$$

and assuming that the discrete current filaments are oriented only in z-direction in cylindrical coordinates, we get:

$$\vec{H}(t) = \sum_{\xi} i_{a\xi}(t) \cdot \frac{\rho_{i\xi}}{4\pi\rho_{\Delta\xi}^{2}} \cdot \left[\frac{(z_2 - z_a)}{\sqrt{(z_2 - z_a)^2 + \rho_{\Delta\xi}^2}} - \frac{(z_1 - z_a)}{\sqrt{(z_1 - z_a)^2 + \rho_{\Delta\xi}^2}} \right] \cdot \begin{pmatrix} -\sin(\varphi - \varphi_{i\xi}) \\ \frac{\rho_a}{\rho_{i\xi}} - \cos(\varphi - \varphi_{i\xi}) \end{pmatrix} \qquad (9)$$

where:

- $\rho_{i\xi}$ - distance of the ξth filament to the origin
- $\rho_{\Delta\xi}$ - projection of the distance of the ξth filament to the sensor in the ρ-φ-plain
- ρ_a - distance between sensor and origin in the ρ-φ-plain
- z_a - distance between sensor and ρ-φ-plain in z-direction
- z_1 - beginning of integration interval in z-direction
- z_2 - end of integration interval in z-direction
- $\varphi - \varphi_{i\xi}$ - difference between angles of the ξth filament and the sensor in the ρ-φ-plain

The unknown currents $i_{a\xi}$ can be calculated solving the system of equations:

$$\left[\vec{G}\right]_{mn} \cdot \left[i_a\right]_n = \left[\vec{H}\right]_m \qquad (10).$$

The quantity m corresponds to the number of probe positions along the aperture.

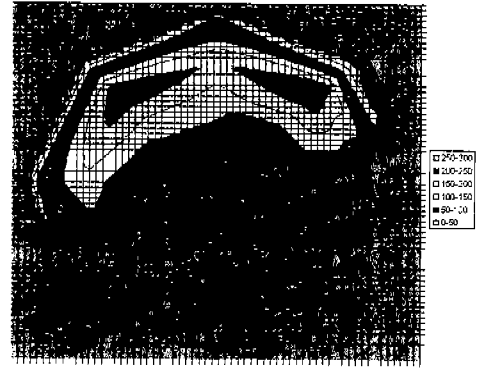

Fig. 7: Measured current density distribution for a GTO carrying 1kA

Tasks of this type are inverse problems of the field calculation, whose solutions are naturally not unique. Instead, one is limited to determining the most probable solution vector by means of iterative solution of the forward problem or least square methods.

Fig. 7 shows the result of a field measurement and analysis of this kind for a steady-state current density distribution. The GTO used was partially irradiated to obtain a controlled local carrier lifetime reduction.

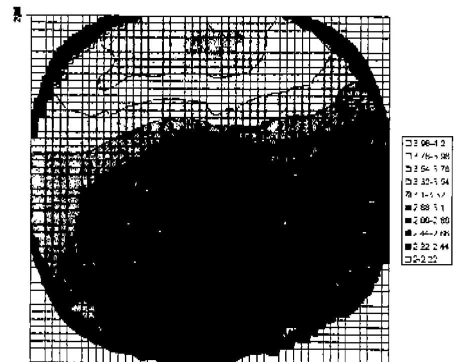

Fig. 8: Measured storage time constant distribution (determined via automatic probing system)

The essential electrical data of the GTOs and their

lateral distributions were analyzed by automatic probing on the individual n^+-emitter fingers of the GTO. As depicted in Fig. 8 the device shows a short storage time in the lower section. Consequently the forward voltage is large in this area. The result is a small current density. However, a non- irradiated part of the GTO in the center of the upper area shows a large storage time and a small forward voltage drop, although the measured current density is not as high as expected in this area. As a further result, the local distribution of the trigger current on the GTO tablet was available. Here even the area described last, shows a higher trigger current. This could explain the relatively small current density in an area, which is extremely well conductive. Thus one of the fundamental design rules in the semiconductor technology can be validated by this small example: The scattering of all device parameters over the active surface must be minimized which maximizes the current the component can turn-off.

5. CONCLUSIONS

A setup has been designed and established to investigate the turn-on and turn-off characterisitcis of high power semiconductor devices. The realized concept separates the capacitance in two parts: one part for the LC resonant circuit and the other one supply the blocking voltage for the DUT during turn-off. By this arrangement the tester needs only half of the capacitance a dc chopper of the same capacity would require. The feedback-network allows an energy economic operation. The tester is able to withstand a DUT failure without damage.

The tester was applied for different transient measurements of high power GTOs. From these measurements the model parameters are extracted for a GTO device. As an example the determiantion is outlined of the high injection lifetime in the n-base from the anode tail current characterisitics. Other GTO parameters are extracted by similar routines from non destructive measurements. The setup also renders an optimization of a parameter set by analyzing the device behavior resulting from a variation of the current and voltage slopes

The tester was improved to enable the measurement of the current density distribution across the device during the turn-off process. A set of concentric rogowski coils detects the transient radial current density distribution. The method of magnetic field strength measurements is applied to test the azimuthal variation of the current density. A comparison between the local current density distribution and the local distribution of the storage time constants of a partial irradiated GTO shows a close correlation. A homogeneous current density distribution is obtainable by a homogeneous regulation of all parameters on the whole device.

ACKNOWLEDGEMENT

The authors would like to thank Prof. Wolfgang, Dr. Türkes, Dr. Lehnert and Dr. Sölkner for fruitful discussions as well as Mrs. Bommersbach for experimental support.

REFERENCES

[1] A. Thiede, "Dimensionierung und Bau eines Laborversuchsstandes zur Messung des Schaltverhaltens von GTO-Thyristoren", Forschungsbericht, TU-Dresden, 1994

[2] L. Göhler, "Thyristormodellierung", Dissertation, Universität der Bundeswehr, 1997

[3] M. Bayer, R. Kraus, A new analytical SCR-model for circuit applications", IEEE Symposium on Power Electronics Circuits (SPEC), Hong Kong, 25-26 July 94, pp. 45-47

[4] Metzner, D.; Otto, J.; Schulze, H.-J.: Non-destructive evaluation of the circuit-dependent turn-off limits of gate turn-off thyristors by the detection of the local current density; IEEE Int. Symp. On Power Semiconductor Devices and ICs, Weimar, Germany,1997, pp.85-88

[5] D. Schröder, "Leistungselektronik – Simulation", ETG-Fachbericht 72, Bad Nauheim, 1998

[6] C. Mark Johnson, Andre`A. Jaecklin, Patrick R. Palmer, Peter Streit, "Correlation Between Local Segment Characteristics and Dynamic Current Redistribution in GTO Power Thyristors", IEEE Transactions on Electron Devices, Vol. 41, No. 5, 1994, pp. 793-798

[7] P.R. Palmer, C.M. Johnson, "Measurement of the Redistribution of Current in GTO Thyristors during turn off", Proceedings of the EPE Aachen, 1989, pp. 1621-1625

[8] P.R. Palmer, C.M. Johnson, "Non destructive Measurements for analyzing Power Semiconductor Devices", Proceedings of 1992 International Symposium on Power Semiconductor Devices & ICs, Tokyo, pp. 8-14

[9] L. Göhler, Th. Langer, J. Sigg, "A destruction free parameter extraction scheme for GTO models", IEEE Industry Application society Annual Meeting (IAS'98), St. Louis, Oct. 12-15, 1998